Available online at www.sciencedirect.com
SCIENCE DIRECT®
Journal of Computational Physics 205 (2005) 626–639
JOURNAL OF COMPUTATIONAL PHYSICS
www.elsevier.com/locate/jcp

Comprehensive boundary method for solid walls in dissipative particle dynamics

D.C. Visser *, H.C.J. Hoefsloot, P.D. Iedema

University of Amsterdam, Faculty of Science, Nieuwe Achtergracht 166, 1018 WV, Amsterdam, The Netherlands

Received 24 August 2004; received in revised form 11 November 2004; accepted 22 November 2004
Available online 19 December 2004

Abstract

Dissipative particle dynamics (DPD) is a particle-based mesoscopic simulation technique, especially useful to study hydrodynamic behaviour in the field of complex fluid flow. Most studies with DPD have focused on bulk behaviour by considering a part of an infinite region using periodic boundaries. To model a finite system instead, boundary conditions of the solid walls confining the system must be addressed. These conditions depend on the time and length scales of phenomena studied, i.e., the level of coarse graining. Here we focus on a mesoscopic level at which small scale atomistic effects near the wall are no longer visible. At this, more macroscopic, level a solid wall should be impenetrable, show no-slip and should not affect the fluid properties. Solid walls used in previous studies were unable to meet all three these conditions or met them with limited success. Here, we describe a method to create solid walls that does satisfy all requirements, producing the correct boundary conditions. The introduction of periodic conditions for curved boundaries makes this new wall method fit for curved geometries as well. And, an improved reflection mechanism makes the walls impenetrable without causing side effects. The method described here could also be implemented in other particle-based models.

Keywords: Dissipative particle dynamics; Boundary conditions; Solid walls

1. Introduction

The rheology in some flow problems, such as complex fluid or multiphase flow, depends on microscopic information of the fluids present. Often, only a low-level of molecular behaviour is relevant and should be captured by the numerical technique employed. Conventional continuum-based techniques are based on

* Corresponding author. Tel.: +31 20 525 5265; fax: +31 20 525 5604.
E-mail addresses: visser@science.uva.nl (D.C. Visser), piet@science.uva.nl (P.D. Iedema).

0021-9991/$ - see front matter © 2004 Elsevier Inc. All rights reserved.
doi:10.1016/j.jcp.2004.11.020

solving the Navier–Stokes equations and have difficulties to address effects on a microscopic scale. On the other hand, molecular dynamics simulations give a full description on atomistic scale that is too detailed and computationally very expensive. Mesoscopic simulation methods that are applicable in between microscopic and macroscopic time- and length-scales, are therefore particularly useful in these situations. Dissipative particle dynamics (DPD) is a particle-based form of such a mesoscopic method. DPD was introduced by Hoogerbrugge and Koelman [1] to study suspensions [2]. Later, the hydrodynamic behaviour in various other problems has been studied with DPD, involving polymers [3], multiple phases [4–6], and heat transfer [7].

Most of these studies simulate part of an infinite region using a system confined by periodic boundaries. Simple shear flow with a linear velocity profile is obtained in such systems with the Lees–Edwards boundary condition [8]. However, systems addressing more complex flow patterns or impenetrable boundaries require real solid walls. The desired behaviour of a solid wall, and hence the boundary conditions, depends on the scale at which a system is observed. On an atomic level it is likely that a wall induces structure in the fluid, as well as locking and slip, influencing the behaviour in the order of nanometers from the wall [9–12]. Nevertheless, when DPD is employed as particle-based flow solver at a mesoscopic level of micrometers, the degree of coarse graining is too high to show such atomistic effects near the wall.

The central question of the present work is how to construct a solid wall for this higher, more macroscopic, level of mesoscopic modelling. On this level three boundary conditions hold for a solid wall: (1) impenetrability; no particles are allowed to enter the wall, (2) no-slip; the wall should impose the correct velocity, and (3) the wall should not affect the fluid properties in the system. Previous studies managed to implement impenetrability and no-slip boundary conditions, but proved to show small scale effects like ordering near the wall, which affects a substantial portion of the system. Obviously, this is not correct from our "macroscopic" point of view, since the properties of a system should not change when a wall is placed around it.

In this paper we present a new method for constructing solid walls solving the problem of the above mentioned wall effects and related anomalies. The method is based on a novel periodic approach that utilizes a set of identical systems, instead of a single one. Besides, a technique is introduced to achieve the correct interaction across a curved boundary, making it possible to model systems with curved walls. Furthermore, we improved the reflection mechanism that guarantees the wall's impenetrability. Together with the existing knowledge about boundary conditions this leads to a comprehensive boundary method for solid walls in DPD.

2. Dissipative particle dynamics

The DPD method describes a fluid system in a coarse-grained fashion by dividing it up in small interacting fluid packages. Each package is represented by a DPD particle that is assumed to show the collective dynamic behaviour of the group of molecules it contains. The evolution of the positions ($\mathbf{r}_i$) and impulses ($\mathbf{p}_i$) of all interacting particles over time is governed by Newton's second law of motion:

$$\frac{\partial \mathbf{r}_i}{\partial t} = \mathbf{v}_i(t), \quad \frac{\partial \mathbf{v}_i}{\partial t} = \mathbf{f}_i(t), \tag{1}$$

where the mass is left out since we will work with particle masses of 1 for simplicity. The equations of motion are solved using the modified velocity-Verlet algorithm presented by Groot and Warren [13]. The total force acting on a particle i is composed of three pairwise additive forces, a dissipative ($\mathbf{F}_{ij}^{\mathrm{D}}$), random ($\mathbf{F}_{ij}^{\mathrm{R}}$) and conservative force ($\mathbf{F}_{ij}^{\mathrm{C}}$)

$$\mathbf{f}_i(t) = \sum_{j \neq i} \left(\mathbf{F}_{ij}^{\mathrm{D}} + \mathbf{F}_{ij}^{\mathrm{R}} + \mathbf{F}_{ij}^{\mathrm{C}} \right). \tag{2}$$

Particles interact only with particles that are within a certain cut-off radius r_c. The degree of interaction depends on the absolute distance r_{ij} between particle i and j. In the mathematical expression for the forces the r_{ij}-dependency is taken into account by so called weight functions $\omega(r_{ij})$.

The dissipative or drag force is related to the velocity difference between the particles and acts as a resistance against motion. It is given by

$$\mathbf{F}_{ij}^{\mathrm{D}} = -\gamma \omega^{\mathrm{D}}(r_{ij})(\hat{\mathbf{r}}_{ij} \cdot \mathbf{v}_{ij})\hat{\mathbf{r}}_{ij}. \tag{3}$$

Here, $r_{ij} = |\, \mathbf{r}_i - \mathbf{r}_j \,|$, $\hat{\mathbf{r}}_{ij} = (\mathbf{r}_i - \mathbf{r}_j)/r_{ij}$, $\mathbf{v}_{ij} = \mathbf{v}_i - \mathbf{v}_j$ and γ is a friction or drag factor. The random force introduces the Brownian-like, chaotic character of molecules and follows as:

$$\mathbf{F}_{ij}^{\mathrm{R}} = \sigma \zeta_{ij} \omega^{\mathrm{R}}(r_{ij}) \hat{\mathbf{r}}_{ij}, \tag{4}$$

in which σ defines the fluctuation amplitude and ζ_{ij} is a random number drawn from a uniform distribution with zero mean and Δt^{-1} variance, where Δt is the time step in the simulation. With the condition $\zeta_{ij} = \zeta_{ji}$ the opposing character of the force between particle pairs remains intact, ensuring conservation of momentum in the model. The conservative force is a soft repulsive force representing the effective potential between the groups of fluid molecules assembled in the different DPD particles. The expression is given by

$$\mathbf{F}_{ij}^{\mathrm{C}} = a \omega^{\mathrm{C}}(r_{ij}) \hat{\mathbf{r}}_{ij}, \tag{5}$$

where a is the maximum repulsion between a pair of particles.

Español and Warren [14] have shown that the system relaxes to a Gibbs–Boltzmann equilibrium distribution when the correct thermostat is applied. They proved that this holds true if the random and dissipative forces are balanced and related to the system temperature T according the fluctuation–dissipation theorem:

$$\omega^{\mathrm{D}}(r_{ij}) = [\omega^{\mathrm{R}}(r_{ij})]^2, \quad \sigma^2 = 2 k_{\mathrm{B}} T \gamma, \tag{6}$$

where k_{B} is the Boltzmann constant. The weight functions, tending to zero for $r_{ij} \to r_c$, can have the following simple form:

$$\omega^{\mathrm{R}}(r_{ij}) = \omega^{\mathrm{C}}(r_{ij}) = \begin{cases} 1 - \frac{r_{ij}}{r_c} & \text{if } r_{ij} < r_c, \\ 0 & \text{if } r_{ij} \geqslant r_c. \end{cases} \tag{7}$$

The simulations in this paper are performed with $r_c = 1.0$, $k_{\mathrm{B}}T = 1.0$, $\sigma = 3.0$, $a = 75/\rho$ and $\Delta t = 0.01$, after the example of Groot and Warren [13]. All measurements are preceded by an equilibration period and all quantities are in arbitrary DPD units, e.g. length is in r_c units.

3. Flat solid walls in DPD

So far only few studies dealt with the construction of solid walls in DPD. Most of them modelled flat walls by locally freezing the DPD particles [15–20], similar to the way solid objects such as colloidal particles are constructed [2,21,22]. The frozen particles interact as normal fluid particles, but have a fixed position and velocity, i.e., the wall velocity. To prevent particles from entering the wall region Kong et al. [15], and Malfreyt and Tildesley [16] chose a higher particle density in the wall, while Jones et al. [17] increased the repulsive force from the wall particles. Both these techniques result in a strong wall repulsion and a depletion of particles near the wall in non-ideal systems ($a > 0$). Later the idea of reflecting the particles

in the wall boundary was introduced to guarantee the wall's impenetrability [19,20]. Nevertheless, a high wall density is still required to approach no-slip in systems with flow as shown by Revenga et al. [20], again producing undesirable density distortions near the wall. Moreover, the frozen positions of the wall particles in these methods intrinsically invoke ordering of particles in the vicinity of the wall, causing density fluctuations and affecting the fluid behaviour near the wall. It should again be realized that such phenomena near the wall should not be visible on the coarse grained level we aim at.

A new method was introduced by Willemsen et al. [24] who imposed the no-slip boundary condition by continuing the velocity profile in an extra layer of particles outside the simulation box. The positions and velocities of the particles in this wall layer are determined from the particles within the interaction distance of the wall. The high spatial correlation between this *no-slip* layer and the system disturbed the particle distribution close to the wall. To avoid this they calculated the repulsive interaction from a different, second layer of particles. By constructing this *repulsive* layer from the layer of particles just outside the interaction distance of the wall the authors tried to achieve an undisturbed particle distribution. However, their method still affects the fluid properties significantly and, thus, violates one of the boundary conditions for a solid wall we pursue here.

The effect of the *Willemsen* method is demonstrated in Fig. 1 for three particle densities ρ in the system, where the particle and velocity distributions are visualized by density and temperature profiles, respectively. The results are obtained for a rectangular system of 6000 particles confined between walls at $x = 0$ and $x = 5$ after averaging over 2×10^4 time steps. No external forces are acting on the system so fluid and walls are at rest. A bounce-back reflection, recommended by Revenga et al. [20], with inversion of the acceleration (see Section 5) makes the wall impenetrable. In such a static situation a periodic boundary shows, apart from impenetrability, the desired wall behaviour: an average velocity of zero and no distortions near the wall. This allows us to observe the effect of the repulsive and the no-slip wall layers from the Willemsen method separately. First, only the repulsive layer is applied, while the dissipative and random interactions are obtained from a periodic image of the system. Then, the no-slip layer is applied, while the repulsive interactions are calculated from a periodic image.

A strong effect of the repulsive layer is observed on the density as well as the temperature. The no-slip layer has no visible effect on the density (not shown in Fig. 1(a) for clarity) and a relatively small but not negligible effect on temperature. Note that for low densities the distortion close to the wall influences the whole system. The distortions are not an effect of time step size and occur also at other equilibrium temperatures. Although the distortions decrease for higher particle densities in the system, they are still not

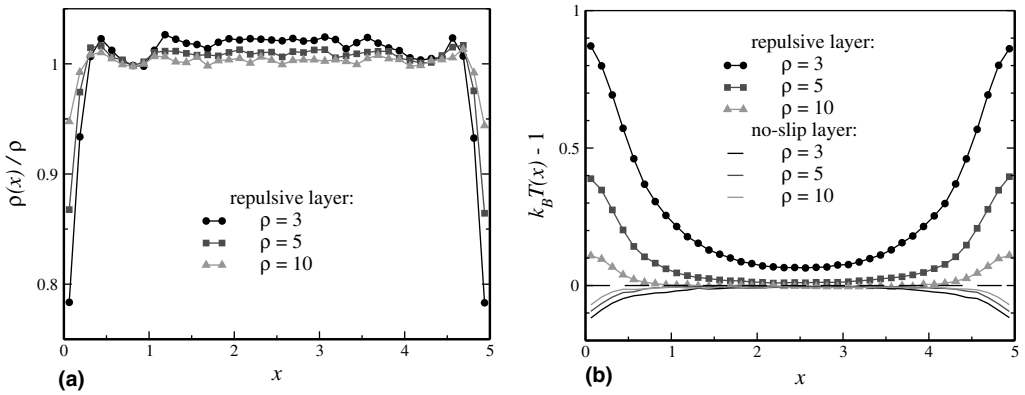

Fig. 1. Effect of the repulsive and no-slip wall layers from the Willemsen method on the density (a) and temperature (b) in different systems.

negligible up to a depth of $0.5r_c$ from the wall for $\rho = 10$. Considering a cubic simulation box of $10 \times 10 \times 10$ the effected region is already 27% of the total simulated volume for $\rho = 10$ and even higher for lower densities. To reach a level at which the wall effects can be neglected, either the system must be enlarged to impractical dimensions, or restricted to very high densities. Both these options are computationally costly and undesirable.

3.1. The parallel wall method

In a single phase DPD system with periodic boundaries the particle and velocity distribution is uniform throughout the system, ensuring homogeneous inter-particle forces in the whole system without undesired distortions at the boundary. Considering the particles within the interaction radius of a periodic boundary, it is observed that they interact directly with particles of the periodic image across the boundary, as if they were normal neighbours. And, just as holds for normal neighbours; action is reaction. Thus, the positions and velocities of particles on both sides of the boundary are directly correlated. This direct correlation across the boundary is lost in the wall method of Willemsen et al. and is apparently the origin of the observed distortions.

An obvious way to acquire direct correlation is to utilize the principle of a periodic boundary in the construction of a wall, as is done for instance in the Lees–Edwards method [8]. The Lees–Edwards method can, however, only be applied to induce shear flow between two parallel walls moving in opposite direction. In other, more complex, situations the flow conditions on both sides of the system are no longer proportional and/or independent of the position along the wall. This makes it impossible to match the periodic images in the Lees–Edwards method without discontinuities in the particle and velocity distribution. Such discontinuities will give rise to distortions and slip.

In view of the foregoing discussion one can see that direct correlation and continuity of the particle and velocity distribution are necessary across the boundary to prevent undesired distortions. Therefore, such characteristics are essential ingredients for the modelling of a solid wall. Lets consider the particle distribution. An obvious way to achieve continuity in the particle distribution across the wall boundary is by mirroring the particle positions over that boundary. This creates a mirror image of the system on the other side of the wall boundary. Applying this mirror image as wall will, however, cause a too strong correlation between the particle positions in the wall and the system [24]. A better option is, instead of using the mirror image of the system itself, to employ the mirror image of a twin system. The dimensions and properties of the twin systems are similar as well as the flow conditions inside. So, in fact, they model the same flow with another set of interacting particles. Parallel calculation of the twin systems guarantees that the particle and velocity distribution in both systems corresponds at any time. Now, placing these parallel twin systems back-to-back, as illustrated in Fig. 2 with systems 1 and 2, they can act as a wall for each other, automatically producing continuity of the particle distribution and direct correlation across the wall boundary. Reflecting the particle velocities of the parallel twin system with respect to the wall velocity in all directions continues the velocity profile beyond the wall, as illustrated in Fig. 2 with arrows, and produces no-slip [24].

The use of multiple systems in this *parallel* wall method seems computationally costly. However, each system provides useful data for the statistical post-process which, in turn, allows one to reduce the sampling space and/or time. Consider, for instance, a rectangular system of $5 \times 10 \times 5$ confined between flat walls at $x = 0$ and $x = 5$. To model the walls in this system with the parallel wall method we need two systems of $5 \times 10 \times 5$, as illustrated in Fig. 2 with system 1 and 2. Seemingly this doubles the computational load. However, both systems model the same flow problem and system 1 and 2 can, in fact, be regarded as two halves of one large system of size $5 \times 10 \times 10$ or $5 \times 20 \times 5$. Thus, to obtain results of the same precision with a system of $5 \times 10 \times 5$ takes twice as long or requires a system that is twice as large. So altogether the parallel wall method takes no additional computation time. An advantage of the parallel wall method over other wall methods is the fact that no extra particles are added to physically construct the wall. Such wall

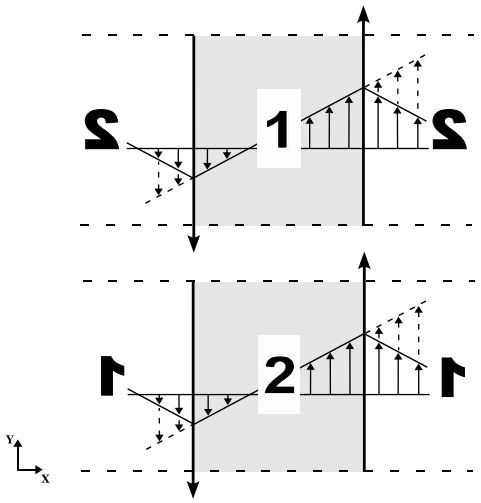

Fig. 2. Schematic drawing to illustrate the parallel wall method for a system with walls in the x-direction. Mirror images (blank) of one parallel system (grey) act as wall for the other and vice versa.

particles do not provide useful information and are therefore inefficient. For the system of $5 \times 10 \times 5$ with walls at $x = 0$ and $x = 5$ the number of extra wall particles the Willemsen method requires is already 40% of the particles present in the system itself. The extra computation time is of the same order. Another computational advantage is that the parallel systems are very suitable for parallel calculation.

To test the effect of the parallel wall method on the fluid properties we performed simulations in a rectangular system of 6000 particles ($\rho = 5$) confined by walls at $x = 0$ and $x = 5$. Again the walls are at rest and a bounce-back reflection with inversion of the acceleration is performed whenever a particle crosses the wall boundary. The boundaries in the y- and z-direction of the simulation box are periodic. At present we check the overall wall performance by observing the mean force on the particles over time at different positions between the walls. An incorrect wall performance will reveal itself directly by an imbalanced, non-zero effective force. In Fig. 3 the effective force profile resulting from the parallel wall method is compared to those resulting from the Willemsen method and periodic boundary conditions after averaging over 2×10^4 time steps. The performance clearly improves when the parallel wall method is used, showing the

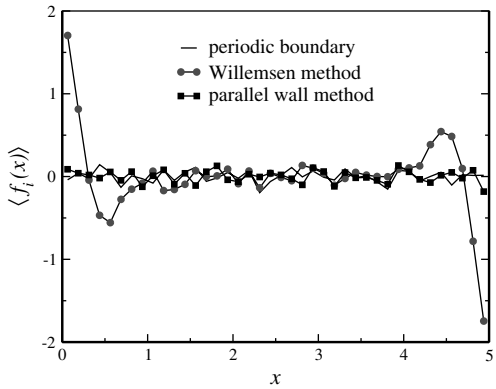

Fig. 3. Effective force as function of the x-position in the system, $\langle f_i(x) \rangle$, resulting from different boundary methods.

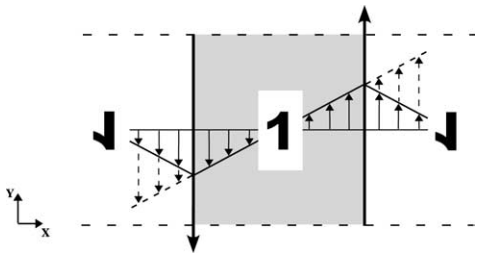

Fig. 4. Schematic illustration of the periodic wall method for a system with walls in the x-direction. The mirrored periodic image (blank) of the system itself (grey) acts as wall.

same uniformity in forces throughout the system as a periodic boundary. Consequently, the strong effect on density and temperature is also absent.

3.2. The periodic wall method

In some special cases we can use a simplified form of the parallel wall method. When symmetry exists in the flow pattern, the required matching particle and velocity distribution can be found within the system itself. Then, the desired wall performance can simply be obtained from a periodic image, and is it not necessary to employ an additional parallel system. This method is, henceforth, referred to as the *periodic* wall method. It is for instance applicable when the walls in Fig. 2 move with the same speed in opposite direction. In such a situation, mirroring the periodic image (of the system itself) in the direction of the wall displacement creates the desired matching on both sides of the system, as illustrated schematically in Fig. 4. Other suitable examples in this respect are Poiseuille flow and systems where the walls move with the same speed in the same direction. In these situations the flow conditions on both sides of the system match exactly and the wall can be constructed directly from the periodic image.

3.3. Walls in more than one dimension

In the methods employed to define a boundary in DPD care must be taken that a particle never interacts with itself and no more than once with another to prevent spurious correlations. As for periodic boundaries, this restricts the parallel and periodic wall method to systems where the wall boundaries are at least r_c and $2r_c$ apart, respectively. It also implies that multiple parallel systems are required when a system is confined by walls in two or three directions. With walls in two directions, for instance, a particle in the corner of the simulation box interacts with three systems across a wall boundary. Like each particle the corner particle should feel particles within its interaction radius that are all different. In the parallel wall method this can only be guaranteed, if the three systems across the wall boundary are three different parallel systems. Hence, a total of four systems should be simulated. Fig. 5(a) illustrates how these systems are matched in the parallel wall method. For the same reason, a set of eight systems is required, when the domain is confined by walls in all directions. Often, though, a plane of symmetry is present in the flow, which enables us to halve the number of required systems by applying the periodic wall method.

Once again no-slip is produced by continuing the velocity profile across the wall boundaries inside the parallel systems. It is obvious that parallel system 2 in Fig. 5(a) sets up the right wall and parallel system 3 the top wall for system 1. Parallel system 4 sets up the wall corner and can be understood as part of the right wall or part of the top wall. This makes it unclear which wall velocity the particles of corner system 4 should impose. The most simple option is to split the corner system in two, grouping the particles to the nearest wall and let them impose the velocity of that wall. However, this will lead to interactions across the top wall

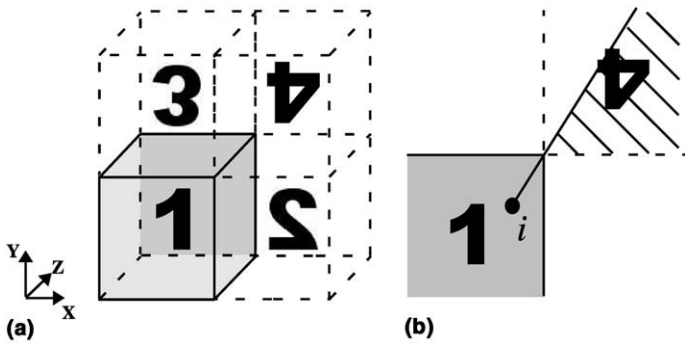

Fig. 5. On the left the back-to-back placement in the parallel wall method is shown for a system with walls in the x- and y-direction. On the right corner system 4 is divided into a region that belongs to the right wall (hatched) and top wall (blank) for particle i of system 1: (a) placement; (b) division.

with particles of the right wall and vice versa. More consistent is, therefore, to assign particles in a corner system to the wall across which they interact. The particles in system 4 are, thus, assigned to the right or top wall based on the position of the particles in system 1, as shown schematically in Fig. 5(b) for particle i. The straight line from i through the point where system 1 and 4 touch divides corner system 4 into a part that belongs to the right and the top wall for this particle.

4. Curved solid walls in DPD

As far as we know, there is only one report in literature concerning curved walls in DPD [23]. The curved walls in that study exist by means of a bounce-back reflection alone, without (frozen) particles physically constructing it. This method results in an accumulation of particles at the wall, instead of a depletion, and similar density distortions as the flat high density walls of frozen particles. The new boundary method for solid walls introduced in Section 3 would offer a good alternative here, but refers to flat walls. In this section we will present a technique that makes them fit for curved walls as well.

In the parallel and periodic wall method the walls are formed, respectively, by the mirror image of a parallel system and the periodic image of the system itself. The presence of a curved boundary makes it impossible to connect the system to such mirror or periodic images in a close-fitting manner. This means that there will be undesirable gaps. However, such a close connection can be recovered by folding the image around the curved boundary. When symmetry is present the periodic mirror image of the system itself can be employed or else the mirror image of a parallel system. The folding procedure is illustrated in Fig. 6(a) for a cylindrical geometry with coordinates (r,θ,z). The cylinder has a radius of R_{cyl} and is infinite in the z-direction. The figure shows the cross-section through the cylinder, marked by the thick black line, and the positions of the particles close to its curved boundary. Since the cylinder is axisymmetric the periodic wall method can be applied, i.e., constructing the wall from the periodic image of the system. However, to prevent particles from interacting with themselves across the boundary a periodic *mirror* image should be employed here instead of a periodic image. Fig. 6(a) shows a part of the periodic mirror image, drawn in grey. It is obtained by placing the cylinder and its periodic image next to each other and mirroring the particle positions of the periodic image in the plane $\theta = 0$. Now, the layer of particles within the interaction radius r_c from the boundary of the periodic mirror image can be folded around the curved boundary of the original system, yielding the desired close connection. Observing the transition of particle j to its periodic mirror image j' to j'' after folding, it becomes clear that the whole folding procedure is, in fact, nothing else than

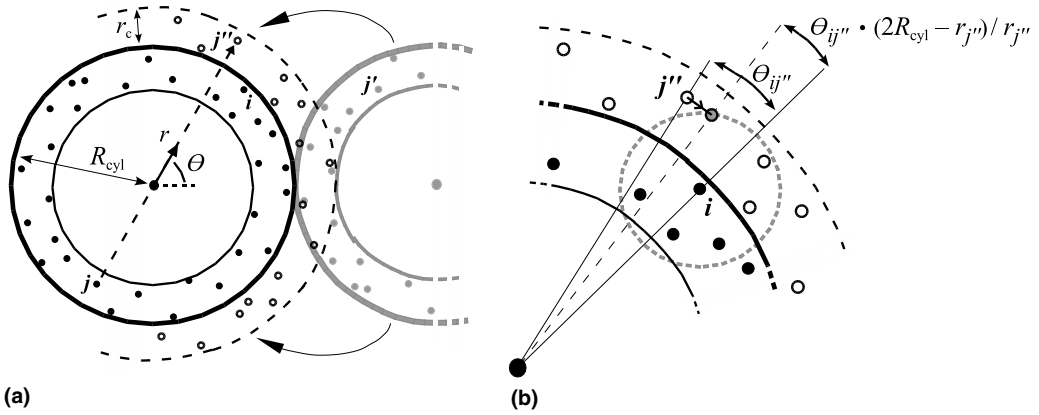

Fig. 6. Schematic representation of the folding (a) and scaling (b) procedures to obtain the correct interaction across a curved boundary. The filled black dots are system particles within the interaction radius of the curved boundary. The unfilled black dots are the positions of the particles across the boundary after folding.

making the system periodic in the direction perpendicular to the boundary. This direction is, in this case, equal to the radial direction, because the radius of curvature R_κ is constant, and equal to the radius of the cylinder.

Nevertheless, folding a curved image around a curved exterior alters the interparticle distances, and thus the particle density, inside that image as a function of curvature and distance perpendicular to the system boundary. The resulting density difference across the boundary will hamper the correct wall behaviour in our wall methods. By scaling the positions of the particles across the wall boundary for every interaction with a system particle we can compensate for the alterations. Scaling of particle positions should only be performed in the tangential direction along the wall, because the interparticle distances normal to the wall stay unchanged during the folding operation. Fig. 6(b) illustrates the scaling procedure for a cylindrical system by observing the interaction between system particle i and particle j'' across the boundary. The number and magnitude of interactions a particle i near the curved boundary experiences are restored to normal bulk values by scaling the positions of all particles across that boundary in the direction along the boundary and relative to the position of i. While the θ-coordinate gives the position along the cylinder's boundary the scaling rule has the following form:

$$\theta_{ij}^{\text{scaled}}(R_\kappa, \Delta_{jw}) = \theta_{ij} \cdot \frac{R_\kappa - \Delta_{jw}}{R_\kappa + \Delta_{jw}} = \theta_{ij} \cdot \frac{2R_{\text{cyl}} - r_j}{r_j}, \tag{8}$$

where θ_{ij} is the distance between a system particle i and a particle j across the boundary in the θ-direction, Δ_{jw} is the distance of particle j normal to the wall and r_j is the radial position of particle j. In Fig. 6(b) scaling places particle j'' just within the interaction range of particle i, which nullifies the effect introduced by the folding step. Similar to flat walls, no-slip at curved walls is obtained by continuing the velocity profile across the boundary, and impenetrability by a reflection mechanism. In Section 6 the no-slip condition at curved walls is tested for the gravity driven flow through a cylindrical tube.

The curvature in two dimensions (e.g. a sphere) is described by two radii of curvature and, using spherical coordinates (r,θ,ϕ), requires scaling in both the θ- as well as the ϕ-direction. Particles are, still, prohibited to feel another particle twice within their interaction radius. The method described in this section is, thus, only sound when the radius of curvature is larger than r_c. Note that this technique is applicable for all sorts of curved boundaries.

5. The reflection mechanism

In the parallel and periodic wall method the walls are formed by images of twin systems or the system itself. Therefore, the wall region differs in no way from the fluid region and nothing prevents the particles to leave the system and enter the wall. For an impenetrable solid wall this should be avoided, which can be realized by reintroducing the particles that cross the wall boundary into the system. Revenga et al. [20] investigated different reintroduction mechanisms and found that only a bounce-back reflection produces the no-slip boundary condition. Although this is still true for the wall methods we introduced here, the current definition of this reflection leaves room for improvements.

First of all, the algorithms solving the equations of motion require the particle's position, velocity and acceleration. The change of these quantities during a reflection should, therefore, be defined. To our knowledge, previous studies only considered the change in position and velocity during the reflection process. When the acceleration of reflected particles is left unchanged after a bounce-back, we observe a significant temperature distortion close to an impenetrable boundary, i.e., the area where the reflections take place. However, when the direction of the acceleration is inverted, just as the velocity, these anomalies are absent. This is shown in Fig. 7, where we plotted the temperature in the region $0.1r_c$ from an impenetrable boundary at rest for different densities in the system. Clearly, inverting the direction of the acceleration is the preferred strategy during a reflection step. With this stated, the definition of the reflection mechanism is complete.

Furthermore, it should be noted that a bounce-back reflection places the particles back in an unnatural, and in some cases unfortunate, fashion. Just as in real systems the DPD particles tend to migrate to a more favourable position, minimizing the energy in the system. However, a bounce-back reflection reverses this motion, redirecting a particle towards the less favourable position. This discrepancy has no consequences when walls exist in one dimension, but induces an artificial and self-enhanced build up of particles when the fluid flows in the direction of a wall confined corner. This is a situation occurring for example in a lid driven cavity, where the moving lid forces the particles towards the corner of the cavity. The pressure will increase and a large number of particles will jump out of the system at this corner. These particles are systematically placed back by the bounce-back mechanism in the unfavourable high pressure corner. The probability that these particles leave the system in the next time step, followed by another reintroduction, is high. Thus, we see that the particles are more or less trapped in the corner region. A solution is offered by a thorough analysis of the bounce-back method, which reveals that its no-slip action relies on the velocity treatment and positioning perpendicular to the wall. This allows a more straightforward and natural positioning that

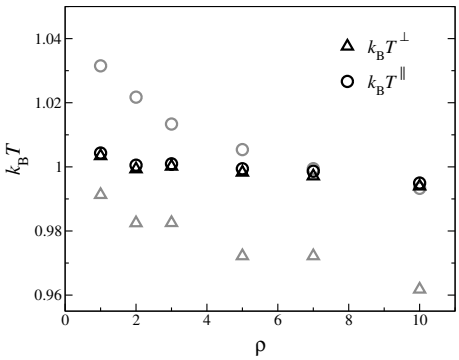

Fig. 7. Temperature close to an impenetrable boundary for bounce-back reflections with (black symbols) and without (grey symbols) inversion of the acceleration. The temperature component perpendicular ($k_BT^{\perp}$) and parallel ($k_BT^{\parallel}$) to the boundary is shown.

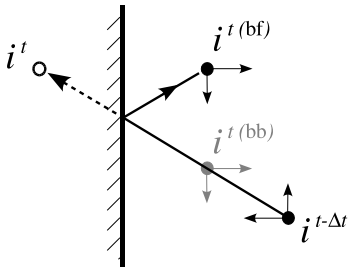

Fig. 8. Bounce-forward ($i^{t(bf)}$) versus bounce-back ($i^{t(bb)}$) reflection for a particle i that jumps out of the system in a time step Δt.

preserves the displacement tangential to the wall during a reflection, while the position perpendicular to the wall and the velocity change according the original bounce-back mechanism as shown in Fig. 8. This *bounce-forward* shows the same no-slip as a bounce-back, as will be shown in Section 6, but cancels the unrealistic accumulation of particles in the corner of a lid driven cavity.

6. The new boundary method put into practice

In this section the new boundary method for solid walls is put into practice. First, we verify if this new method complies with the no-slip boundary condition. Then, we calculate the development of a velocity profile in two different geometries, a rectangular geometry with flat walls and a cylindrical geometry with curved walls.

6.1. No-slip boundary condition

The new boundary method is tested with respect to the no-slip condition by computing the steady velocity profile for the shear flow between flat walls. The left wall at $x = 0$ is at rest, while the right wall at $x = 10$ is moving at a constant speed $V_z^{\text{wall}} = 2.00$. In this situation, the amount of velocity slip at the walls V^{slip} depends on the distance L_x between the walls and the imposed shear rate V_z^{wall}/L_x. The simulated velocity profiles are linear in the whole region between the walls. Therefore, we defined V^{slip} as V_z^{wall} minus the slope of the calculated velocity profile times L_x, where the slope is determined by means of linear regression. Fig. 9 shows the amount of slip for different densities in the system. A small amount of slip is observed at low

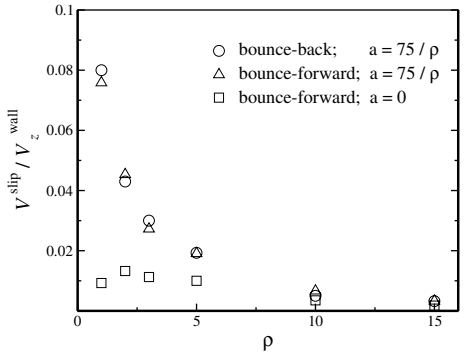

Fig. 9. Performance of the new boundary method for solid walls with respect to the no-slip condition at different densities in the system.

densities that depends on the fluid's compressibility. For ideal system ($a = 0$) slip is negligible over the whole density range. Fig. 9 shows also that bounce-back and bounce-forward reflections have the same effect on the no-slip condition.

6.2. Flow between flat and curved walls

The development of a velocity profile in two typical flow situations is calculated. In the first situation the left wall of a rectangular system is instantaneously set in motion with a constant velocity $V_z^{\text{wall}} = 2.00$. In the second situation a gravitational force of $g = 0.08$ is switched on in a cylindrical system. The fluid, initially at rest, is accelerated in both cases until a steady laminar flow is reached. Theoretical solutions exist for the velocity distribution of the time dependent start-up process as well as the steady-state [25].

Simulations are performed with a set of 120,000 particles ($\rho = 5$) between walls that are $10r_c$ apart in case one ($L_x = 10$) and a wall with a radius of curvature equal to $10r_c$ in case two ($R_{\text{cyl}} = 10$). The kinematic viscosity ν of these systems (required in the theoretical solutions) has a value of 0.257 and is computed from a stationary shear flow simulation (see for instance [8]) using Lees–Edwards boundary conditions. Case one requires the parallel wall method while the symmetric flow pattern in case two permits the application of the periodic wall method for curved boundaries as described in Section 4. Therefore, two parallel systems of 60,000 particles are used in the first situation and a single system of 120,000 particles in the second. A bounce-forward reflection with inversion of the acceleration is performed whenever a particle crosses the wall boundary. Fig. 10 plots two start-up velocity profiles and the stationary profile for each situation. All profiles are normalized with the maximal velocity $V_z^{\max}$ of the fully developed theoretical flow. The dimensionless time τ is given by $\nu \cdot t/L_x^2$ for case one and $\nu \cdot t/R_{\text{cyl}}^2$ for case two. The agreement between the simulated and the theoretical profiles is excellent for both the unsteady and steady-states. This proves that the solid walls constructed with the new boundary method yield the correct velocities in instationary situations. It also shows that the correct velocity is imposes at curved walls, validating our technique to implement curved boundaries. The undisturbed density and temperature profiles in both flow situations (not shown here) confirm once more that the walls have no effect on the fluid properties.

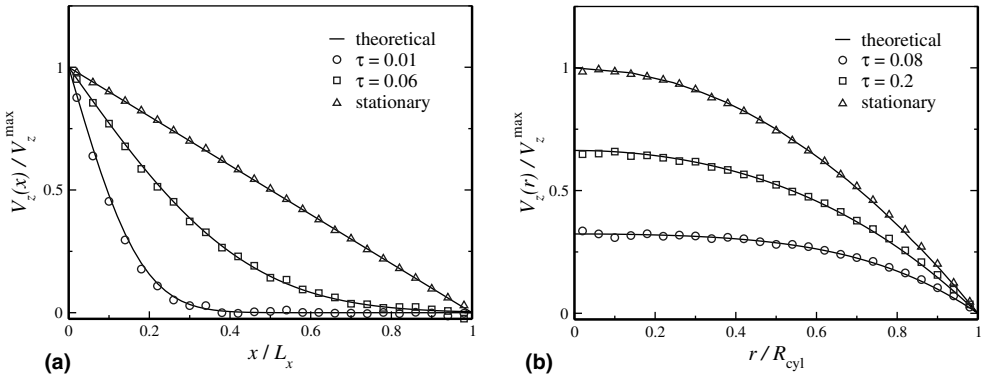

Fig. 10. Comparison of simulated (symbols) and theoretical (lines) velocity distributions for the velocity development in two flow situations with different geometry: (a) flow between flat walls; (b) flow through a tube.

7. Discussion

In this paper we studied the wall behaviour in a single phase system where the wall is constructed from the same material as the fluid. In reality the wall material differs and has its own specific interactive forces. As a result, the phases in a multiphase system may have a different affinity with the wall. Such a microscopic phenomenon has a macroscopic effect on the interface between and transport behaviour of the fluids present. It is, for instance, responsible for the rise of the water interface near a glass wall. We may expect that adsorption/desorption, motion and contact angle of droplets or fluid portions are strongly influenced by the interaction with the wall. Incorporation of the wall material in the solid wall method is, thus, of special importance for multiphase systems and a next challenge.

Although the present work employs the DPD simulation technique, the introduced new wall method could also be applied in other particle-based techniques like smoothed particle hydrodynamics or molecular dynamics. Furthermore, some of our ideas to implement boundary conditions for solid walls could proof valuable in the construction of solid objects such as colloids.

8. Conclusion

The objective of our work was to improve the modelling of solid walls in the dissipative particle dynamics simulation technique. Therefore, we introduced a new wall construction method that makes use of parallel twin systems which set up the wall by a back-to-back placement. This automatically generates a smooth particle and velocity distribution across the wall boundary as well as correct interparticle correlations. Hence, we are able to simulate a wall that meets the no-slip boundary condition without affecting the properties of the system. To make our new wall method applicable to curved boundaries, we developed a folding and scaling procedure to connect curved systems with their periodic image or the image of a parallel system. This allows one to model curved walls as well. A bounce-back reflection ensures the wall's impenetrability but it may introduce side effects. If the tangential displacement to the wall is left unaltered for particles that are reintroduced, the bounce-back method transforms into a bounce-forward method that shows the same no-slip but lacks these side effects. Both reflection methods leave the thermodynamics of the system intact when the acceleration of a particle is changed in opposite direction after a reflection. The new boundary method meets all requirements for solid walls at higher densities, but shows some velocity slip at low densities for non-ideal systems. Correcting this flaw as well as constructing solid walls for multiphase systems are future challenges.

Acknowledgments

This work is part of the OSPT research program *Computational fluid dynamics of disperse multiphase flows*. Financial support by AKZO Nobel Chemical Research, DSM Research and Shell Global Solutions International B.V. is gratefully acknowledged.

References

[1] P.J. Hoogerbrugge, J.M.V.A. Koelman, Simulating microscopic hydrodynamics phenomena with dissipative particle dynamics, Europhys. Lett. 19 (1992) 155–160.

[2] J.M.V.A. Koelman, P.J. Hoogerbrugge, Dynamic simulation of hard-sphere suspensions under steady shear, Europhys. Lett. 21 (1993) 363–368.

[3] A.G. Schlijper, P.J. Hoogerbrugge, C.W. Manke, Computer simulation of dilute polymer solutions with the dissipative particle dynamics method, J. Rheol. 39 (1995) 567–579.
[4] K.E. Novik, P.V. Coveney, Using dissipative particle dynamics to model binary immiscible fluids, Int. J. Mod. Phys. C 8 (1997) 909–918.
[5] S.M. Willemsen, T.J.H. Vlugt, H.C.J. Hoefsloot, B. Smit, Combining dissipative particle dynamics and Monte-Carlo techniques, J. Comput. Phys. 147 (1998) 507–517.
[6] R.E. Van Vliet, H.C.J. Hoefsloot, P.J. Hamersma, P.D. Iedema, Pressure-induced phase separation of polymer-solvent systems with dissipative particle dynamics, Macromol. Theory Simul. 9 (2000) 698–702.
[7] S.M. Willemsen, H.C.J. Hoefsloot, D.C. Visser, P.J. Hamersma, P.D. Iedema, Modelling phase change with dissipative particle dynamics using a consistent boundary condition, J. Comput. Phys. 162 (2000) 385–394.
[8] M.P. Allen, D.J. Tildesley, Computer Simulation of Liquids, Clarendon Press, Oxford, 1987.
[9] D.Y.C. Chan, R.G. Horn, The drainage of thin liquid films between solid surfaces, J. Chem. Phys. 83 (1985) 5311–5324.
[10] E. Watts, J. Krim, A. Widom, Experimental observation of interfacial slippage at the boundary of molecularly thin films with gold substrates, Phys. Rev. B 41 (1990) 3466–3472.
[11] J. Koplik, J.R. Banavar, J.F. Willemsen, Molecular dynamics of fluid flow at solid surfaces, Phys. Fluid A 1 (1989) 781–794.
[12] P.A. Thompson, M.O. Robbins, Shear flow near solids: epitaxial order and flow boundary conditions, Phys. Rev. A 41 (1990) 6830–6837.
[13] R.D. Groot, P.B. Warren, Dissipative particle dynamics: bridging the gap between atomistic and mesoscopic simulation, J. Chem. Phys. 107 (1997) 4423–4435.
[14] P. Español, P.B. Warren, Statistical mechanics of dissipative particle dynamics, Europhys. Lett. 30 (1995) 191–196.
[15] Y. Kong, C.W. Manke, W.G. Madden, A.G. Schlijper, Simulation of a confined polymer in solution using the dissipative particle dynamics method, Int. J. Thermophys. 15 (1994) 1093–1101.
[16] P. Malfreyt, D.J. Tildesley, Dissipative particle dynamics simulations of grafted polymer chains between two walls, Langmuir 16 (2000) 4732–4740.
[17] J.L. Jones, M. Lal, J.N. Ruddock, N.A. Spenley, Dynamics of a drop at a liquid/solid interface in simple shear fields: a mesoscopic simulation study, Faraday Discuss. 112 (1999) 129–142.
[18] A.T. Clark, M. Lal, J.N. Ruddock, P.B. Warren, Mesoscopic simulation of drops in gravitational and shear fields, Langmuir 16 (2000) 6342–6350.
[19] J.B. Gibson, K. Zhang, K. Chen, S. Chynoweth, C.W. Manke, Simulation of colloid-polymer systems using dissipative particle dynamics method, Mol. Simul. 23 (1999) 1–41.
[20] M. Revenga, I. Zúñiga, P. Español, I. Pagonabarraga, Boundary models in DPD, Int. J. Mod. Phys. C 9 (1998) 1319–1328.
[21] E.S. Boek, P.V. Coveney, H.N.W. Lekkerkerker, Computer simulation of rheological phenomena in dense colloidal suspensions with dissipative particle dynamics, J. Phys.: Condens. Matter 8 (1996) 9509–9512.
[22] E.S. Boek, P.V. Coveney, H.N.W. Lekkerkerker, P. van der Schoot, Simulating the rheology of dense colloidal suspensions using dissipative particle dynamics, Phys. Rev. E 55 (1997) 3124–3133.
[23] J.R. Darias, M. Quiroga, E. Medina, P.J. Colmenares, R. Paredes V, Simulation of suspensions in constricted geometries by dissipative particle dynamics, Mol. Simul. 29 (2003) 443–449.
[24] S.M. Willemsen, H.C.J. Hoefsloot, P.D. Iedema, No-slip boundary condition in dissipative particle dynamics, Int. J. Mod. Phys. C 11 (2000) 881–890.
[25] R.B. Bird, W.E. Stewart, E.N. Lightfoot, Transport phenomena, Wiley, New York, 1960.